

# Evaluation of the static magnetic field interactions for a newly developed magnetic ophthalmic implant at 3 Tesla MRI

## Untersuchung der Wirkungen eines statischen Magnetfeldes auf ein neu-entwickeltes magnetisch ophthalmologisches Implantat in einem 3 Tesla MRT

### Authors

Ann-Kathrin Bodenstein<sup>1</sup>, Matthias Lüpke<sup>1</sup>, Christian Seiler<sup>1</sup>, Frank Goblet<sup>1</sup>, Stephan Nikolic<sup>2</sup>, Ulf Hinze<sup>3</sup>, Boris Chichkov<sup>4</sup>, Claudia Windhövel<sup>5</sup>, Jan-Peter Bach<sup>5</sup>, Lisa Harder<sup>5</sup>, Hermann Seifert<sup>1</sup>

### Affiliations

- 1 Institute for General Radiology and Medical Physics, University of Veterinary Medicine Hannover, Foundation, Hannover, Germany
- 2 eye clinic at Aegi, Augenärzte am Aegi, Hannover, Germany
- 3 Nanotechnology Department, Laser Zentrum Hannover e.V, Hannover, Germany
- 4 Laboratory of Nano and Quantum Engineering, Leibniz Universität Hannover, Germany
- 5 Small Animal Clinic, University of Veterinary Medicine Hannover, Foundation, Hannover, Germany

### Key words

ophthalmologic implant, magnetic resonance imaging, MRI safety, magnetic forces

received 29.11.2017

accepted 06.06.2018

### Bibliography

DOI <https://doi.org/10.1055/a-0690-9050>

Published online: 11.10.2018

Fortschr Röntgenstr 2019; 191: 209–215

© Georg Thieme Verlag KG, Stuttgart · New York

ISSN 1438-9029

### Correspondence

Ann-Kathrin Bodenstein

Fachgebiet Allgemeine Radiologie und Medizinische Physik,  
Tierärztliche Hochschule Hannover, Bischofsholer Damm 15,  
Haus 102, 30173 Hannover, Germany

Tel.: ++49/05 11/8 56 72 95

[ann-kathrin.bodenstein@tiho-hannover.de](mailto:ann-kathrin.bodenstein@tiho-hannover.de)

### ABSTRACT

**Purpose** The purpose of this study is to analyze the static magnetic field interactions for an ophthalmic-magnetic shunt implant with a ferromagnetic steel plate in a thin silicon layer. The plate is used for opening of a valve flap. Ten different sizes of this steel plate were investigated to characterize the relationship between the size of the metal and the magnetic forces of the static magnetic field of a 3.0 T MRI.

**Materials and Methods** The magnetic translation force  $F_z$  was quantified by determining the deflection angle using the deflection angle test (ASTM F 2052). The torque was qualitatively estimated by using a 5-point grading scale (0: no torque; +4: very strong torque) according to Sommer et al. [11]. For the visual investigation of the function of the metal plate both prototypes were positioned at the magnetic field's spatial gradient and at the magnet's isocenter. The stitches were exposed to the thousandfold of the translational force by a dynamometer.

**Results** The translational force was found to be 10 times greater than the weight of a single plate. The plates were exposed to a high torque (grade 3 to 4). The seams and the tissue withstood more than a thousandfold of the determined translational force. No spontaneous, uncontrolled opening of the valve flap was visible in the MRI, as a result of which the intraocular pressure could decrease considerably.

**Conclusion** Due to the small size of the plates the translational force and the torque will be compensated by the silicon layer and also by the fixation in the eye.

### Key points:

- Magnetic forces will be compensated by silicon layer and fixation in the eye.
- The magnetic-ophthalmological implant is not restricted in its function by the MRI magnetic field.
- The ophthalmic magnetic shunt implant can be considered conditionally MRI-safe.

### Citation Format

- Bodenstein A, Lüpke M, Seiler C et al. Evaluation of the static magnetic field interactions for a newly developed magnetic ophthalmic implant at 3 Tesla MRI. *Fortschr Röntgenstr* 2019; 191: 209–215

### ZUSAMMENFASSUNG

**Ziel** Das Ziel dieser Studie ist es, die Wirkungen eines statischen Magnetfeldes während einer MRT-Untersuchung auf ein magnetisch-ophthalmologisches Implantat *in vitro* zu bestimmen. Das Implantat besteht aus Silikon und einem eingebetteten Metallplättchen, das zur Öffnung einer Ventilklappe dient. Es wurden zehn unterschiedliche Größen des Metallplättchens untersucht, um die Abhängigkeit der magnetischen Kräfte von der Größe des Metallplättchens zu charakterisieren.

**Material und Methode** Es wurden 10 Metallplättchen mit Größen zwischen  $8 \times 8 \text{ mm}^2$  und  $1 \times 1 \text{ mm}^2$  und 2 Prototypen des Implantats an einem 3 Tesla-MRT untersucht. Im statischen Magnetfeld wurde die Translationskraft mithilfe des Fadentests (ASTM F 2052) und das Drehmoment anhand einer

5-Punkte-Graduierung nach Sommer et al. [11] bestimmt (Grad 0: kein Drehmoment, Grad 4: starkes Drehmoment). Die beiden Prototypen wurden im Bereich des höchsten Feldgradienten der Translationskraft und im Isozentrum des MRTs dem Drehmoment ausgesetzt und das Verhalten der Ventilklappe wurde visuell auf Funktionalität untersucht. Zusätzlich wurden mit einem Kraftmesser die Fixierungsnähte des Implantats und das Skleragewebe des Auges dem tausendfachen der errechneten Translationskraft ausgesetzt.

**Ergebnisse** Die Translationskraft war in der Regel fast 10-mal so groß wie die Gewichtskraft  $F_G$  eines Plättchens. Die Metallplättchen waren einem starken Drehmoment ausgesetzt (Stufe 3 bis 4). Die Nähte und das Gewebe hielten mehr als dem Tausendfachen der ermittelten Translationskraft stand. Im MRT war kein spontanes, unkontrolliertes Öffnen der Ventilklappe sichtbar, in dessen Folge der Augeninnendruck stark abnehmen könnte.

**Schlussfolgerung** Durch die geringe Größe, die Silikonummantelung und die Fixation durch die Nähte können die Translationskraft und das Drehmoment kompensiert werden.

## 1. Introduction

As a diagnostic method, magnetic resonance imaging (MRI) is used for imaging soft tissue structures. During an MRI examination, ferromagnetic materials in the patient's body can become a potential danger to the patient. The high magnetic field strength can result in movement of the implant, causing irreversible damage to sensitive organs such as the eye [1]. The literature has frequently described the risks and physical interactions of ferromagnetic objects in MRI [2–6]. The purpose of this study is to investigate the behavior of an implant under development in a 3 T MRI unit. This implant is primarily used to treat glaucoma and is positioned in a pre-prepared scleral pocket in the eye. It consists of a silicone base body into which a microvalve flap containing a ferromagnetic plate is cut. There is a small gap between the valve and the base body through which a constant outflow of aqueous humor is achieved, thus preventing the development of excessive intraocular pressure. An external magnet is used to regularly open the valve to prevent attachment of fibroblasts. Fibrosis and associated closure is often a cause of functional failure of conventional glaucoma drainage implants [7, 8].

Due to the widespread clinical use of MRI, it is very important to check the MRI suitability of new implants. Therefore the study will examine *in vitro* the magnetic forces acting on an implant.

## 2. Materials and Methods

### 2.1 Material

All tests were performed on a 3 T MRI unit (Philips, Achieva 3.0 T TX). Two prototypes were examined *ex vivo*, which were implanted in the eye in the region of the sclera in the head of a freshly

sacrificed rabbit. Both prototypes consist of a silicone body with a microvalve flap made of chromium-nickel steel with dimensions of  $0.5 \times 0.5 \text{ mm}^2$  and a thickness of  $50 \mu\text{m}$ . The two prototypes differ from one another with respect to their shape and the number of suture points used to fix the implant in the intraocular tissue in the area of the sclera. Prototype 1 is circular with a diameter of 4 mm and was attached at three points in the eye. The silicone body of prototype 2 is rectangular ( $3 \times 2 \text{ mm}^2$ ) and has four suture points.

The properties of the microvalve flaps were determined *in vitro* prior to the investigations. Since a metal plate with a size of  $0.5 \times 0.5 \text{ mm}^2$  can be handled in MRI only with great difficulty, 10 insulated metal plates made of chromium-nickel steel with a thickness of  $50 \mu\text{m}$  and base areas between  $1 \times 1$  and  $8 \times 8 \text{ mm}^2$  were used in the tests (► **Table 1**). The related values for the implant prototypes were extrapolated from the results of these measurements.

### 2.2 Methods

#### 2.2.1 Measurement of translational force

The standardized ASTM F 2052 deflection angle test [9] was used to measure the translational force upon the metal plates, which involved a plate fixed to a non-ferromagnetic holder via a free-swinging string and positioned on the central axis of the MRI in the area of the maximum induced magnetic force (► **Fig. 1a, b**). This region was determined using Kemper's method [10] at the static magnetic field located 86 cm from the isocenter of the magnet. The deflection angle  $\beta$  in the direction of the vertical z-line of the magnetic field was read from the string using a protractor. The translational force  $F_T$  in z-direction (magnetic field

► **Table 1** Overview of the characteristics of the steel plate.

no. of SP	side-length [mm <sup>2</sup> ]	m [mg]	F <sub>G</sub> [mN]
1	8 × 8	23.90	0.234
2	7 × 7	18.50	0.181
3	6 × 6	13.90	0.136
4	5 × 5	9.30	0.0912
5	4 × 4	5.80	0.0569
6	3 × 3	3.30	0.0324
7	2 × 2	1.10	0.0108
8	1.5 × 1.5	0.70	0.00687
9	1.25 × 1.25	0.50	0.00491
10	1 × 1	0.40	0.00392
11 <sup>1</sup>	0.5 × 0.5	0.10	0.000981

SP – Steel Plate; m – mass; F<sub>G</sub> – weight forces.

<sup>1</sup> extrapolated values of steel plate 11.

direction) was calculated for each metal plate based on each angle of deflection according to

$$F_T = F_G \times \tan(\beta) = m \times g \times \tan(\beta) \quad (1)$$

Thus F<sub>G</sub> denotes the weight force, m the mass of the metal plate, g the acceleration due to gravity (9.81 m/s<sup>2</sup>) and β the deflection angle in relation to the vertical.

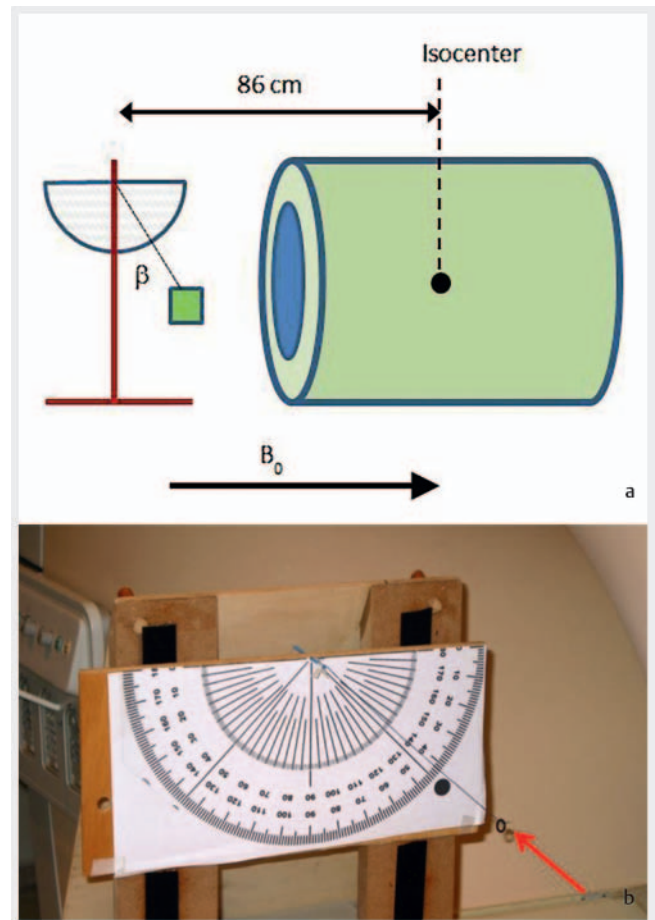
The implants were additionally weighted with rubber or plastic loads weighing between 0.052 g and 0.440 g to achieve a deflection angle between 25° and 65°. Each metal plate was measured twice with two different weights. The mean translational force was then determined and compared with the weight force F<sub>G</sub>.

### 2.2.2 Torque determination

Torque M was determined following an internationally-established standard method [11 – 13], likewise in a static magnetic field. A laminated protractor was positioned horizontally in the isocenter of the magnet. Each metal plate was then individually put on the protractor and placed in positions of 45°, 90°, 135°, 180°, 225°, 270° and 315° to B<sub>0</sub> (► Fig. 2). Two observers analyzed how each metal plate reoriented itself to the magnetic field B<sub>0</sub>. This movement was qualitatively evaluated using a 5-point graduation according to Sommer et al. [11] (► Table 3).

### 2.2.3 Checking the functionality of the magnetic valve flap

In order to demonstrate the functionality of the implant prototypes (see section 2.1), the opening of the flap of each prototype was visually checked with a neodymium magnet (magnetic flux density of 0.5 T at 1 mm axial distance, 0.26 T at 5 mm distance) using a reflected-light microscope. The magnet was held very closely to the magnetic valve flap (distance approx. 1 mm). Prototype 1 implanted in the eye of a rabbit's head was used to check



► **Fig. 1** a Schematic illustration of the translational force apparatus [10]. The deflection angle β is measured to the direction of the magnetic field B<sub>0</sub>. b Translational force apparatus (wooden) with paper protractor and the suture mounting made of plastic. The steel plate (marked by a red arrow) and the additional weight (rubber ring) fixed on a suture.

whether unintentional opening of the flap occurs during MRI. The head was placed in various locations both in the gantry area and in the isocenter of the MRI. Behavior of the flap was observed using a magnifying glass (focal length f = 5 cm) and an MRI-compatible light source.

### 2.2.4 Checking the holding forces on the fixation sutures of the implant

To test the stability of the fixation sutures, prototype 1 was exposed to a force of 10 mN in the eye of a freshly sacrificed rabbit using a dynamometer. A suture (Vicryl Plus, 3 – 0) was placed centrally below the implant. Using the suture and dynamometer, the implant was laterally pulled at an angle of 0° (directly from above), laterally at an angle of 45° and nasally at an angle of 45°. The implant was subjected to the force for 20 minutes in each position. Subsequently the retaining sutures were examined and assessed using a reflected light microscope.

► **Table 2** Overview of the weight forces, translational force and torque of the steel plates in 3 T MRI.

no.of SP	$F_G$ [mN]	$F_T$ average [mN]	$\sigma_{FT}$ [mN]	$F_T/F_G$	M score
1	0.234	2.37	0.21	10.1	4
2	0.181	1.72	0.32	9.47	4
3	0.136	1.26	0.20	9.21	4
4	0.0912	0.722	0.04	7.92	4
5	0.0569	0.505	0.04	8.87	4
6	0.0324	0.298	0.05	9.20	3
7	0.0108	0.0791	0.04	7.32	3
8	0.00687	0.0491	0.03	7.15	3
9	0.00491	0.0354	0.02	7.21	3
10	0.00392	0.0562	0.04	14.3	3
11 <sup>1</sup>	0.000981	0.00981	/	10	/

SP – Steel Plates;  $F_G$  – weight forces;  $F_T$  – translational force;  $\sigma_{FT}$  – standard deviation; M – torque.  
<sup>1</sup> extrapolated values of steel plate 11.



► **Fig. 2** Laminated angle scale with a metallic steel plate positioned on 45°. This position describes the angle between the marker in the middle of the plate towards  $B_0$ .

### 3. Results

#### 3.1 Translational force and torque

The translational force  $F_T$  calculated for the 10 metal plates (MP) lay between 0.0354 mN (MP 9) and 2.37 mN (MP 1) (► **Table 2**). The translational force increased with the size of the plates and was usually almost 10 times as great as the weight force  $F_G$  (► **Fig. 3**). When investigating the torques, the square plates, regardless of their size, showed an orientation with an outer edge parallel to the magnetic field  $B_0$  (► **Table 2**). Plates 1 to 5 showed an immediate and rapid orientation with respect to  $B_0$  (Score 4). Plates 6 to 10 showed a less rapid movement in their preferred direction compared to plates 1 to 5 (Score 3).

► **Table 3** Qualitative evaluation of torque [11].

score 0	no torque	no movements towards $B_0$
score 1	mild torque	the object slightly changes orientation but does not align to $B_0$
score 2	moderate torque	the object aligns directly to $B_0$
score 3	strong torque	the object shows rapid and strong movement to $B_0$
score 4	very strong torque	the object shows very rapid and very forceful alignment to $B_0$

#### 3.2 Functionality of the magnetic valve flap

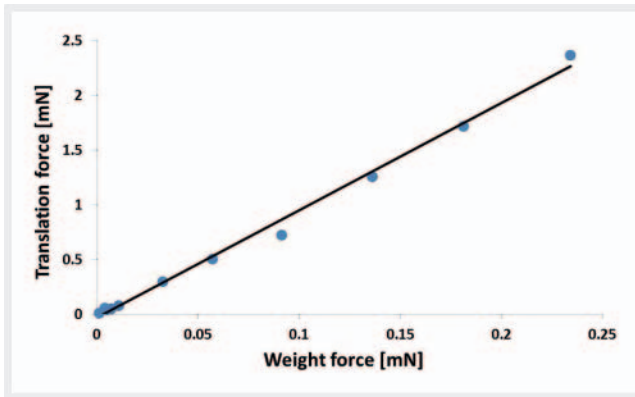
The flaps of prototype 1 and prototype 2 opened when the neodymium magnet approached the implant (distance magnet to implant: about 1 mm). When the influence of the prototype 1 flap on the MRI was checked, the flap did not open in the area of the highest field gradient ( $\leq 17$  T/m [14]) or in the isocenter.

#### 3.3 Implant fixation suture holding forces

During the subsequent microscopic examination, no changes were visible at the fixation points or on the scleral tissue.

### 4. Discussion

This study investigated a new type of magnetic ophthalmological implant regarding its MRI safety with respect to magnetic translational forces and torque. The strength of the forces or torques de-



► **Fig. 3** Translation force as a function of the weight force of the 10 steel plates in a 3 T MRI (gradient of the straight lines: 9.62; coefficient of determination R<sup>2</sup>: 0.99).

depends on the magnetic field gradient, possibly on the magnetizability (= magnetic susceptibility  $\chi$ ) of the material, on the magnetic field strength  $B_0$ , on the mass and position of the implant in the magnetic field as well as on the geometry of the implant [15]. Ferromagnetic metals such as iron, cobalt and nickel are characterized by a high susceptibility (e. g. iron  $\chi_{Fe} \approx 10^5$ ) and are therefore considered to be “MRI unsafe” since they are exposed to large forces in the magnetic field. Likewise, their alloys and many steel grades can also initially be classified as unsafe without precise knowledge of their susceptibility [16].

#### 4.1 Translational force

The maximum translational force is achieved where the product of magnetization and field gradient reaches its maximum. This location is in the region of the gantry opening, since on the one hand the field strength is so high that the material already shows a saturated magnetization, while on the other hand there is a large field gradient due to the divergence of the field lines, and the field gradient goes towards zero. The translational force therefore increases with approach to the gantry opening, reaches a maximum in the area of the opening and disappears within the MRI, as a homogeneous magnetic field is present there. Consequently the patient is exposed to the greatest translational force when passing through the magnet opening [10]. For the investigated metal plates of different sizes, there was a linear relationship between their weight and their translational force. This also demonstrates that all plates have the same composition of chromium and nickel. Each metal plate is subjected to a translational force that is about 10 times greater than its own weight. The deflection angle test used is an established method for determining translational force [2, 17–19]. Without additional weight, the metal plates exhibited a deflection angle of approx. 90°. At a deflection angle of 90°, no calculation of the translational force is possible due to the tangent in equation (1). Therefore, the metal plates were weighted with non-magnetic weights to achieve a

deflection angle of less than 65° [10, 20, 21]. In order to improve the measuring accuracy, the measurements were carried out twice with different weights [22]. According to ASTM guidelines, objects with a deflection angle of more than 45° are classified as “MRI unsafe” [9, 10]. The reason for this is that with these objects, the force acting by the static magnetic field is greater than the gravitational force acting on the object [10, 22]. When evaluating this statement, it must be taken into account that the implant will later be firmly fixed in the eye by sutures. According to Mühlenweg et al. the risk of dislocation decreases with the age of the implantation (>6 months) due to scarring [16]. Even after microsurgical treatment of the sclera, there is a scarring reaction after a few months [23]. Since a very high translational force acts on the implants which is significantly higher than their own weight force, the test described in section 2.2.4 should be reviewed against a worst-case scenario to determine whether the retaining sutures and silicone can counteract the translational force. The metal plate of prototype 1 weighs 0.1 mg. Interpolation of the values in ► **Table 2** yields a translational force of 0.01 mN. The dynamometer used pulled on the implant with a force of 10 mN from different angles for 20 minutes each. On the whole the sutures were exposed to a thousand times the calculated force. Since the subsequent microscopic examination revealed no changes in the position of the sutures, it can be presumed that the implant is not dislocated during the MRI examination, and that both the sutures and the tissue resist force. However, this method does not permit a clear statement whether tractive force at the histological level can cause minor damage or induce inflammation.

#### 4.2 Torque

The strongest torques are to be expected in the isocenter of the magnetic field of an MRI where the magnetic field is most homogeneous and imaging occurs [10]. Depending on the size of the metal plates, the torque score was between 3 and 4 (► **Table 2**), i. e. the diagonals of the plates were oriented with a fast and instantaneous movement parallel to  $B_0$ . The torque score decreased as the dimensions of the plates decreased (► **Table 2**). One reason for this are the lower magnetic moments associated with the smaller dimensions of the plates [16]. The frictional forces between plate and the test surface did not decrease in the same way, so that the frictional forces had a stronger influence on smaller plates, thus reducing the resulting torque [11]. Determination of the torque was methodologically very difficult since there is no uniform method for quantifying the torque for very small objects. Consequently, only a qualitative assessment of torque was performed by two independent observers using a 5-point graduation, which was developed specifically for small objects [10–13, 24, 25]. In contrast to translational force, it is difficult to define an upper safety limit value for torque [11]. Whereas translational force increases linearly with the field strength, torque increases in proportion to the square of the field strength [10], and is therefore a considerable and not specifically calculable safety risk [11]. The torque acting on the implant depends not only on the dimensions

and susceptibility of the material but above all on its geometric shape. In particular, elongated objects are exposed to strong torque, while for square-shaped objects, the torque is usually lower [10]. Although the metal plates in the isocenter of the MRI are exposed to great torque, it is not sufficient to cause opening of the valve flap or displacement of the silicone body.

### 4.3 Functionality

In addition, according to chapter 2.2.3, it was examined whether the magnetic valve flap opens in the MRI or whether its function is restricted. When the implant was positioned in the area of the isocenter and the gantry area, opening of the flap was not visible using a magnifying glass. In contrast, the flaps of both prototype 1 and prototype 2 could be opened with a bar magnet, although it has a smaller magnetic field than the MRI. This can be explained by the fact that the small spatial expanse of the magnet is associated with a large field gradient, while the field gradient is lower due to the extended magnetic field of the MRI. In summary, it can be assumed that the function of the magnetic valve flap is not restricted or disturbed by the translational forces and torques generated by the magnetic field of the MRT.

## 5. Conclusions

Due to the small size of the implant only small forces act on it, which can be easily compensated for by its silicone sheath and suture fixation. An estimation of possible heating is still necessary for a fundamental assessment of the MRI suitability of the implant. This was carried out in a second study together with an investigation of artifact formation.

#### CLINICAL RELEVANCE OF THE STUDY

- Due to the frequent clinical use of MRI, new implants must be tested for their MRI safety.
- Magnetic forces have been precisely evaluated in order to assess the effect of tractive forces.
- The eye, in particular, contains sensitive structures which could incur irreparable damage through dislocation of the implant.
- The function of the magnetic valve flap is not restricted or damaged by the magnetic forces during an MRI examination.

#### Conflict of Interest

The authors declare that they have no conflict of interest.

## References

- [1] Kelly WM, Paglen PG, Pearson JA et al. Ferromagnetism of intraocular foreign body causes unilateral blindness after MR study. *American journal of neuroradiology* 1986; 7: 243–245
- [2] Seibold LK, Rorrer RA, Kahook MY. MRI of the Ex-PRESS stainless steel glaucoma drainage device. *The British journal of ophthalmology* 2011; 95: 251–254
- [3] Davis P, Crooks L, Arakawa M et al. Potential hazards in NMR imaging: heating effects of changing magnetic fields and RF fields on small metallic implants. *American Journal of Roentgenology* 1981; 137: 857–860
- [4] Geffen N, Trope GE, Alasbali T et al. Is the Ex-PRESS glaucoma shunt magnetic resonance imaging safe? *Journal of glaucoma* 2010; 19: 116–118
- [5] Ayyıldız S, Kamburoğlu K, Sipahi C et al. Radiofrequency heating and magnetic field interactions of fixed partial dentures during 3-tesla magnetic resonance imaging. *Oral Surgery, Oral Medicine, Oral Pathology and Oral Radiology* 2013; 116: 640–647
- [6] Biberthaler P. 10 frequently asked questions about magnetic resonance imaging in patients with metal implants. *Der Unfallchirurg* 2009; 112: 521–524
- [7] Choritz L, Wegner M, Förch R et al. Pathophysiology of fibrotic encapsulation of episcleral glaucoma drainage implants. *Der Ophthalmologe* 2013; 110: 714–721
- [8] Thieme H. Newest developments and assessment of epibulbar glaucoma drainage implants. *Der Ophthalmologe* 2013; 110: 712–713
- [9] Philips. Magnetic Resonance, Technical Description, Intera 1.5T Release 2.6.1, Achieva 1.5T / 3.0T / XR Release 2.6.1, Panorama HFO Release 2.6.1. In: Royal Philips Electronics N.V. 2008: 3–7
- [10] Kemper J, Klocke A, Kahl-Nieke B et al. Kieferorthopädische Brackets in der Hochfeld-Magnetresonanztomografie: Experimentelle Beurteilung magnetischer Anziehungs- und Rotationskräfte bei 3 Tesla. *Fortschr Röntgenstr* 2005; 177: 1691–1698
- [11] Sommer T, Maintz D, Schmiedel A et al. Hochfeld-Magnetresonanztomografie: Magnetische Anziehungs- und Rotationskräfte auf metallische Implantate bei 3.0 T. *Fortschr Röntgenstr* 2004; 176: 731–738
- [12] Kangarlu A, Shellock FG. Aneurysm clips: evaluation of magnetic field interactions with an 8.0 T MR system. *Journal of Magnetic Resonance Imaging* 2000; 12: 107–111
- [13] Shellock FG, Kanal E. Yasargil aneurysm clips: evaluation of interactions with a 1.5-T MR system. *Radiology* 1998; 207: 587–591
- [14] Philips. Magnetic Resonance, Technical Description, Intera 1.5T Release 2.6.1, Achieva 1.5T / 3.0T / XR Release 2.6.1, Panorama HFO Release 2.6.1. In: Royal Philips Electronics N.V. 2008: 3–7
- [15] Mühlenweg M, Schaefer G, Trattng S. Sicherheitsaspekte in der Hochfeld-Magnetresonanztomografie. *Der Radiologe* 2008; 48: 258–267
- [16] Mühlenweg M, Schaefer G, Trattng S. Physikalische Wechselwirkungen in der MRT. *Der Radiologe* 2015; 55: 638–648
- [17] Shellock FG, Shellock VJ. Metallic stents: evaluation of MR imaging safety. *American journal of roentgenology* 1999; 173: 543–547
- [18] Williams MD, Antonelli PJ, Williams LS et al. Middle ear prosthesis displacement in high-strength magnetic fields. *Otology & neurotology: official publication of the American Otological Society, American Neurotology Society [and] European Academy of Otology and Neurotology* 2001; 22: 158–161

- [19] Klocke A, Kahl-Nieke B, Adam G et al. Magnetic Forces on Orthodontic Wires in High Field Magnetic Resonance Imaging (MRI) at 3 Tesla. *Journal of Orofacial Orthopedics/Fortschritte der Kieferorthopädie* 2006; 67: 424–429
- [20] New P, Rosen B, Brady TJ et al. Potential hazards and artifacts of ferromagnetic and nonferromagnetic surgical and dental materials and devices in nuclear magnetic resonance imaging. *Radiology* 1983; 147: 139–148
- [21] Kagetsu N, Litt A. Important considerations in measurement of attractive force on metallic implants in MR imagers. *Radiology* 1991; 179: 505–508
- [22] Klocke A, Kemper J, Schulze D et al. Magnetic Field Interactions of Orthodontic Wires during Magnetic Resonance Imaging (MRI) at 1.5 Tesla. *Journal of Orofacial Orthopedics/Fortschritte der Kieferorthopädie* 2005; 66: 279–287
- [23] Sachsenweger M, Klauß V, Nasemann J et al. *Duale Reihe Augenheilkunde*; Thieme; 2002
- [24] Nogueira M, Shellock FG. Otologic bioimplants: ex vivo assessment of ferromagnetism and artifacts at 1.5 T. *American Journal of Roentgenology* 1994; 163: 1472–1473
- [25] Applebaum EL, Valvassori GE. Effects of magnetic resonance imaging fields on stapedectomy prostheses. *Archives of Otolaryngology* 1985; 111: 820–821